Progress In Electromagnetics Research Letters, Vol. 42, 187–199, 2013

DESIGN OF A HIGH POWER, HIGH EFFICIENCY KA-BAND HELIX TRAVELING-WAVE TUBE

Luwei Liu [1], Yanyu Wei [1, *], Yabin Zhang [1], Guoqing Zhao [1], Zhaoyun Duan [1], Wenxiang Wang [1], Yubin Gong [1], and Minghua Yang [2]

[1]National Key Laboratory of Science and Technology on Vacuum Electronics, University of Electronic Science and Technology of China, Chengdu 610054, China

[2]National Key Laboratory of Science and Technology on Vacuum Electronics, Beijing Vacuum Electronics Research Institute (BVERI), P. O. Box 749, Ext Box 41, 100016, China

Abstract—The design and analysis of a high power and high efficiency helix traveling-wave tube operating in the Ka-band are presented. First, a double-slotted helix slow-wave structure is proposed and employed in the interaction circuit. Then, negative phase-velocity tapering technology is used to improve electronic efficiency. From our calculations, when the design voltage and beam current are set to be 18.45 kV and 0.2 A, respectively, this tube can produce average output power over 800 W ranging from 28 GHz to 31 GHz. The corresponding conversion efficiency varies from 21.83% to 24.16%, and the maximum output power is 892 W at 29 GHz.

1. INTRODUCTION

Millimeter-wave radiation sources with wide-bandwidth, high power, and high efficiency are attractive for many applications, such as high-date-rate communications, high-resolution radar, and space applications [1–3]. The helix traveling-wave tube (TWT) is one of the most important millimeter-wave radiation sources due to its outstanding combination of small size, light weight, high efficiency, good linearity, output power and large bandwidth [4]. There are mainly three methods to increase the output power of helix TWT when the

Received 9 July 2013, Accepted 15 August 2013, Scheduled 9 September 2013

* Corresponding author: Yanyu Wei (yywei@uestc.edu.cn).

design voltage and beam current remain constant. The first method is to improve the heat dissipation capability of the slow-wave structure (SWS). The second one is to improve the interaction impedance of the SWS, and the last one is to maintain beam-wave synchronization for a longer period.

So far, several methods have been proposed to improve the heat dissipation capability of the helix SWS, such as by increasing the contact area at helix-rod interface [5, 6] and rod-shell interface [7], by using Diamond rod [8], by using appropriate assemble methods [9–14]. The helix pitch profile is optimized to maintain beam-wave synchronization so that electronic efficiency can be improved, such as positive phase-velocity tapering (PVT) [15, 16] and negative PVT [17–19]. However, there has been less research on how to enhance the interaction impedance.

Recently, a novel slotted helix SWS with high heat dissipation capability [20], as shown in Figure 1(b), has been proposed for developing high power millimeter-wave TWT. This slotted helix SWS, which is derived from the conventional helix SWS, as shown in Figure 1(a), has higher heat dissipation capability, smaller thermal deformation than conventional helix SWS as described in [21, 22]. Here, this novel slotted helix SWS is named as three-slotted helix SWS. While the interaction impedance of the three-slotted helix SWS is a bit smaller than conventional helix SWS, which limits the intensity of the beam-wave interaction. In order to enhance the interaction impedance and meanwhile ensure good heat dissipation capability, a double-slotted helix SWS is proposed. In this paper, we will try to employ this double-slotted helix SWS and negative PVT approach to design a high power, high efficiency Ka-band helix TWT.

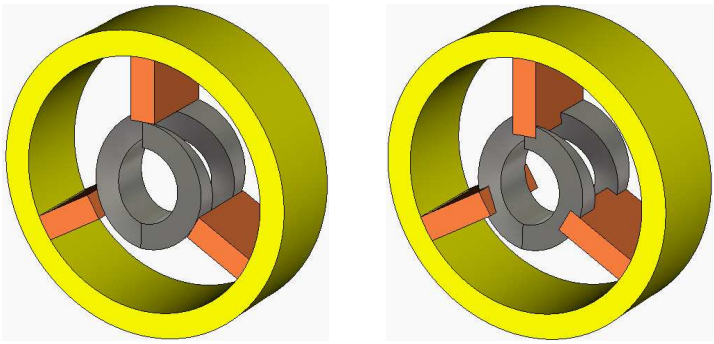

Figure 1. (a) Conventional helix SWS. (b) Three-slotted helix SWS.

This paper is organized in the following manner. Section 1 is a brief introduction. The model of the double-slotted helix SWS is described in Section 2. High-frequency characteristics are calculated in Section 3. The simulation results of the beam-wave interaction of the double-slotted helix TWT operating in the Ka-band are given in Section 4. A brief summary is given in Section 5.

2. THE DOUBLE-SLOTTED HELIX SLOW-WAVE STRUCTURE DESCRIPTION

Figure 2(a) shows the model of the double-slotted helix SWS, which consists of a slotted helix tape, two Beryllium oxide (BeO) dielectric support rods and a slotted metal shell. In this structure, two parallel rows of rectangular slots spaced apart 180° are made in the outside of the helix tape and the inner surface of the metal shell, and all of the four rows of rectangular slots are lined in parallel with the central axis of the helix. Then, the support rods are inserted into the rectangular slots tightly. Because the number of dielectric support rods is reduced, the interaction impedance is increased. Based on the double-slotted helix SWS, high power and high efficiency millimeter wave helix TWTs are expected.

Figure 2(b) shows the dimensional parameters of the double-slotted helix SWS. Here a is the inner radius of the slotted helix tape, b the outer radius of the helix tape, c the inner radius of the shell, d the width of the dielectric support rod, w the width of the helix tape, p the pitch of the helix SWS, and h_1 and h_2 are the depths of the slots in the helix tape and the metal shell.

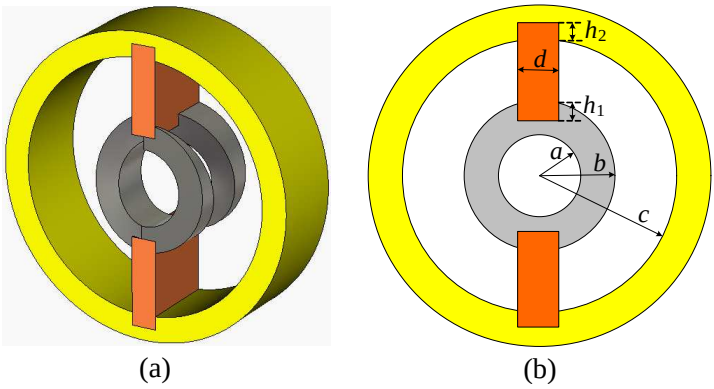

Figure 2. (a) Model of the double-slotted helix SWS. (b) Dimensional parameters of the double-slotted helix SWS.

3. HIGH-FREQUENCY CHARACTERISTICS

The high-frequency characteristics of the double-slotted helix SWS, which include dispersion characteristics, interaction impedance, are calculated by the eigenmode solver with master and slave boundary conditions [23] in the 3-D electromagnetic simulation software Ansoft HFSS [24]. The optimized dimensional parameter values of the double-slotted helix SWS are presented in Table 1. Here, in order to highlight the advantages of the double-slotted helix SWS, the high-frequency characteristics of the conventional helix SWS and the three-slotted helix SWS are also calculated under the condition of the same normalized phase velocity at 30 GHz.

Table 1. Optimized parameters of the double-slotted helix SWS.

Parameter	a/d	c/d	w/a	h_1/h_2	p/b
Value	1.5	4	1.1	1	1.3

Figure 3 shows comparisons of dispersion characteristics and interaction impedance of the fundamental mode at the zero space harmonic among the three helix SWSs. Because the loaded dielectric has a large effect on the dispersion characteristics and interaction impedance in the helix SWS, the more dielectric it contains, the flatter the dispersion curve will be, and meanwhile the lower the interaction impedance will be [25]. The dielectric in the double-slotted helix SWS is less than the other two kinds of helix SWSs, so the dispersion characteristics of the double-slotted helix SWS are the worst and its

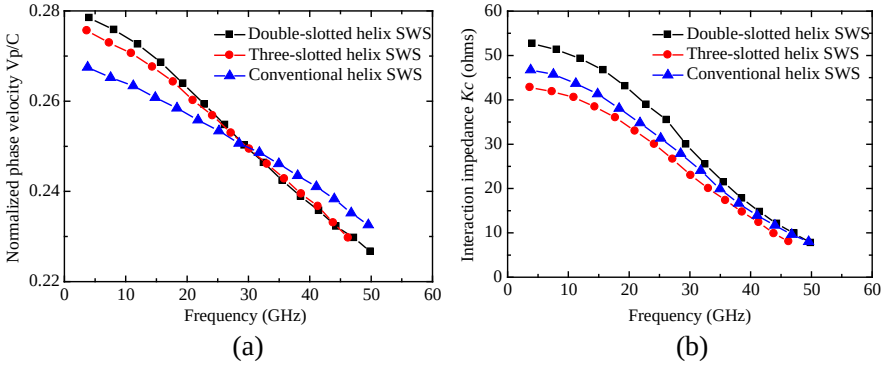

Figure 3. (a) Dispersion characteristics of the three SWSs. (b) Interaction impedance of the three SWSs.

interaction impedance is the largest among the three helix SWSs. While the interaction impedance represents the strength of the beam-wave interaction in the traveling-wave tube [26], so the double-slotted helix SWS can support the strongest beam-wave interaction and output power of the double-slotted helix TWT will be the largest.

4. BEAM-WAVE INTERACTION SIMULATIONS

The transmission characteristics of the double-slotted helix slow-wave circuit have been calculated and optimized by the transient solver in the CST Microwave Studio [27], where the whole circuit length is set as 60 periods. To match the radio-frequency (RF) signal entering into and exiting from the helix circuit, a simple coaxial cable with center conductor equivalent to the width of the helix tape is used as couplers to minimize mismatch. In the simulations, the relative permittivity of the dielectric support rod is 6.5, the conductivity of the double-slotted helix tape is set as 5.8×10^7 S/m. The simulation result is given in Figure 4. It demonstrates that the reflection loss S_{11} is less than -20 dB and transmission loss S_{21} is larger than -0.9 dB over the frequency range of 20∼39 GHz.

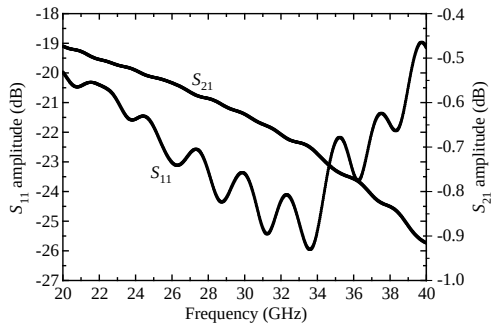

Figure 4. Transmission characteristics of the double-slotted helix slow-wave circuit.

Subsequently, a three-dimensional particle-in-cell model of the double-slotted helix TWT operating in the Ka-band is constructed based on the dimensional parameters obtained above. The beam-wave interaction simulations are carried out by using the PIC solver in the CST Particle Studio [28] to substantiate the amplification capability of the TWT. In order to obtain large gain, the whole interaction circuit is divided into two sections, as shown in Figure 5(a), where the first section consists of 65 periods and the second section

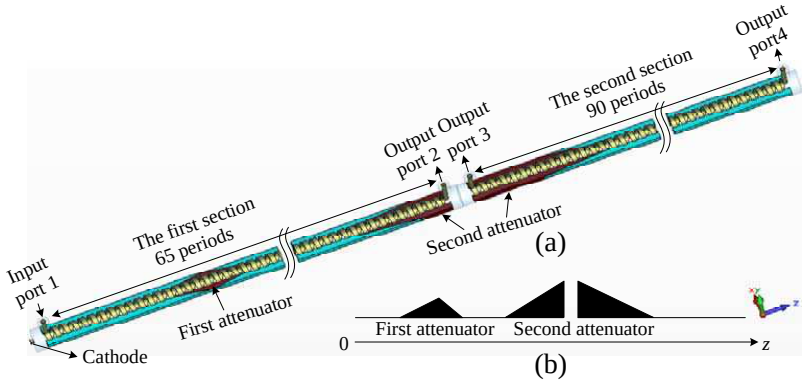

Figure 5. (a) Three-dimensional model of the complete tube. (b) The lower right inset gives the attenuator profile along the interaction length.

consists of 90 periods. Here, output port 2 and output port 3 are the ideal match ports, which can monitor the signal power that has not been absorbed by the concentrated attenuator. These two ports are very helpful to design attenuation of the two attenuators and the length of the whole interaction circuit. To suppress backward wave oscillation and reflection oscillation, two concentrated attenuators made of Carburized porous beryllium oxide with relative permittivity and high loss tangent of 6.5 and 0.5 are used in the interaction circuit, as shown in Figure 5(b). The axial positions of the attenuators are shown in Figure 6. Where, S_1 is the starting position of the first attenuator and S_2 is the starting position of the second attenuator in the first section. The purpose of the first attenuator is to absorb the power of the backward wave and reflection wave in the first section, so the conditions of the backward wave oscillation and reflection oscillation cannot satisfy. The function of the second attenuator in the first section is to absorb the electromagnetic wave completely in the end of the first section or else reflection oscillation can be caused by the reflection wave. While, the function of the second attenuator in the second section is to absorb the power of the backward wave and reflection wave completely, so the conditions of the backward wave oscillation and reflection oscillation cannot satisfy too. In order to absorb the electromagnetic wave, the attenuations of the attenuators in the first section and in the second section are set to be 30 dB and 40 dB, respectively.

In order to improve electronic efficiency, negative PVT approach [17] is used to design the interaction circuit. The whole RF

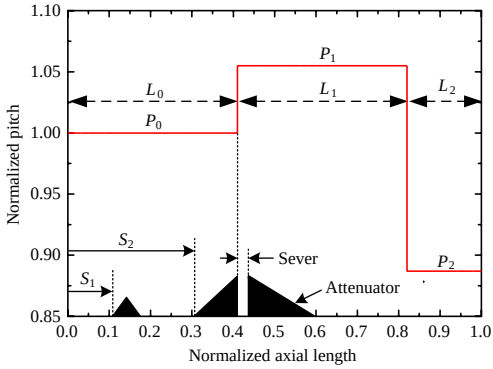

Figure 6. Optimum pitch and attenuator profile versus axial distance of the double-slotted helix TWT.

circuit consists of input section L_0 with pitch P_0 followed by an increased phase velocity section L_1 with pitch P_1 and then a negative tapered section L_2 with pitch P_2, as shown in Figure 6. The purpose of the negative PVT is that the first section L_0 is to obtain the maximum small-signal gain, the section L_1 is to obtain the maximum beam bunching and the section L_2 is to extract the energy from the bunched beam as effectively as possible, so electronic efficiency can be greatly improved.

In the simulations, a pencil electron beam emitted from cathode is injected into the interaction circuit, and the electron beam filling factor is set at 0.65. A uniform longitudinal focusing magnetic field of 0.35 T is employed for the beam focus. Through the optimization calculations, when $p_1/p_0 = 1.055$, $p_2/p_1 = 0.887$, $L_1/L_2 = 2.278$, $S_1/(L_0 + L_1 + L_2) = 0.112$, $S_2/(L_0 + L_1 + L_2) = 0.304$, and the length of the sever is 1 mm, the TWT has the maximum average output power. The optimized operating parameters of the double-slotted helix TWT are shown in Table 2.

Typical simulation results of the double-slotted helix TWT at a representative frequency of 30 GHz are shown from Figure 7 to Figure 9. The time-domain features of the input signal and output signals monitored at input port 1 and output port 4 are shown in Figure 7. It can be seen that after the interaction process of beam-wave, the input signal of 0.33 V is amplified to 41.97 V with electron efficiency of 23.87%. Because the termination is matched very well, the oscillation phenomenon is not observed. Figure 8 gives the frequency spectrum of the output signal obtained from the Fourier transform of electron fields at the output port 4. The output signal spectrum

Table 2. Optimized parameters for a 30-GHz TWT.

Parameter	Value
Beam Voltage	18450 V
Beam Current	0.2 A
Center Frequency	30 GHz
Input power	54.45 mW
Saturated output power	881 W
Saturated gain	42.09 dB
Saturated efficiency	23.87%

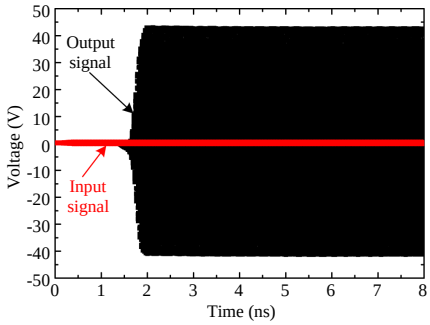

Figure 7. Input signal and output signal at 30 GHz.

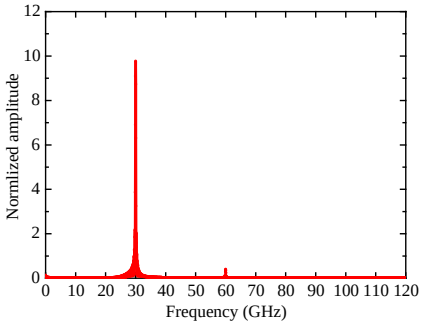

Figure 8. Frequency spectrum of output signals obtained from the Fourier transform of the electron fields monitored at the port 4.

is concentrated around 30 GHz and is relatively pure. Although the higher harmonics are also excited at around 60 GHz, their amplitude is much smaller than that of the operating frequency.

Figure 9 shows the phase momentum plot of the bunched electron beam along the axial distance at 8.0 ns when the electron dynamic system is already in a steady state. It can be seen that the electronic energy in the accelerating zone stops growing at the axial distance of 91 mm and the proportion of electrons in the retarding phase field is increased, which indicates that the negative PVT approach can maintain beam-wave synchronization for a longer period, so the electronic efficiency can be improved very well.

In the same way, the instantaneous bandwidth of this TWT can be calculated with the same input power. Here, for comparison,

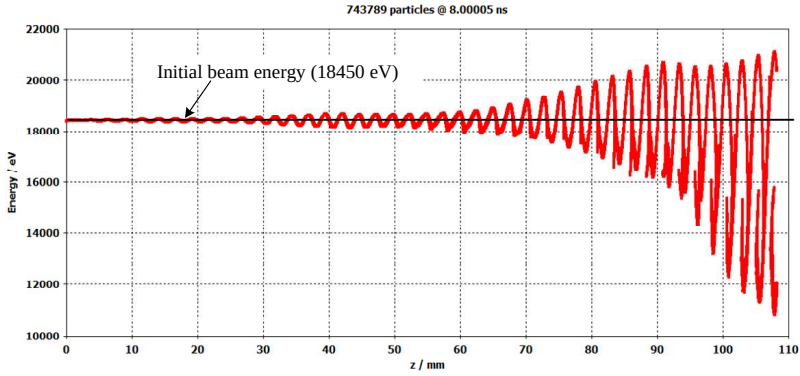

Figure 9. Phase momentum plot of the bunched electron beam at 30 GHz.

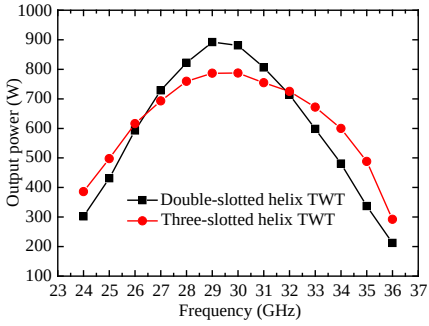

Figure 10. Output power versus frequency.

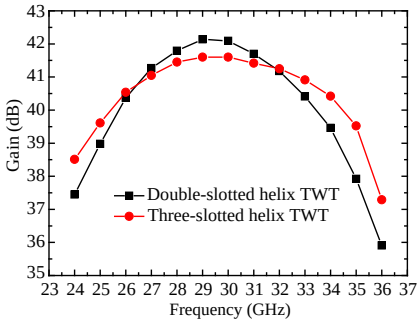

Figure 11. Saturated gain versus frequency.

the interaction performances of the three-slotted helix TWT are also simulated with the same electrical parameters and the same negative PVT approach. The comparisons of the output power, saturated gain and electronic efficiency are illustrated from Figure 10 to Figure 12. As can be seen, the double-slotted helix TWT can produce average output power over 800 W ranging from 28 GHz to 31 GHz and the corresponding conversion efficiency varies from 21.83% to 24.16%, while the three-slotted helix TWT could not. The maximum output power is 892 W at 29 GHz, which is 105 W larger than that of the three-slotted helix TWT. Although the instantaneous 3-dB bandwidth of the double-slotted helix TWT is smaller than three-slotted helix TWT, it can satisfy many applications requiring high power TWTs [29, 30] especially in the frequency range of 28 $\sim$ 31 GHz.

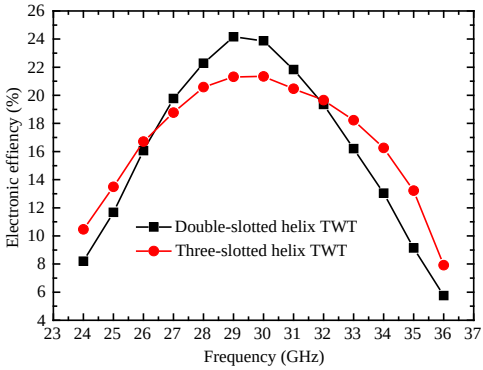

Figure 12. Electronic efficiency versus frequency.

5. CONCLUSION

In conclusion, the double-slotted helix SWS and negative PVT technology have been used to design a high power and high efficiency Ka-band traveling-wave tube. The simulation results show that the double-slotted helix TWT can produce over 800 W average output power ranging from 28∼31 GHz, and the corresponding gain and electronic efficiency can reach over 41.7 dB and 21.83%. In the same electrical parameters and the same negative PVT approach, the maximum output power of the double-slotted helix TWT is 105 W larger than that of the three-slotted helix TWT, so the output power of the double-slotted helix TWT is much more competitive. In addition, because the number of the dielectric support rods is smaller than the conventional helix SWS and the three-slotted helix SWS, the gases released from the dielectric rods due to beam interception are reduced. Therefore, the double-slotted helix SWS is a promising slow-wave structure for developing high power and high efficiency millimeter-wave TWT. Future work will be concentrated on the experimental study of the double-slotted helix TWT.

ACKNOWLEDGMENT

This work was supported by the National Natural Science Foundation of China (61271029), National Science key laboratory found and the National Science Fund for Distinguished Young Scholars of China (Grant No. 61125103).

REFERENCES

1. Chong, C. K., J. A. Davis, R. H. Le Borgne, M. L. Ramay, R. J. Stolz, R. N. Tamashiro, J. P. Vaszari, and X. Zhai, "Development of high-power Ka-band and Q-band helix-TWTs," *IEEE Trans. Electron Devices*, Vol. 52, No. 5, 653–659, May 2005.
2. Qiu, J. X., B. Levush, J. Pasour, A. Katz, C. M. Armstrong, D. R. Whaley, J. Tucek, K. Kreischer, and D. Gallagher, "Vacuum tube amplifiers," *IEEE Microw. Mag.*, Vol. 10, No. 7, 38–51, Dec. 2009.
3. Komm, D. S., R. T. Benton, H. C. Limburg, W. L. Menninger, and X. L. Zhai, "Advances in space TWT efficiencies," *IEEE Trans. Electron Devices*, Vol. 48, No. 1, 174–176, Jan. 2001.
4. Chong, C. K. and W. L. Menninger, "Last advancements in high-power millimeter-wave helix TWTs," *IEEE Trans. on Plasma Science*, Vol. 38, No. 6, 1227–1238, Jun. 2010.
5. Chorney, P., M. E. Hines, and R. J. Madore, "High power slow wave circuit," USA Patent No. 3519964, Jul. 1968.
6. Pchelnikov, Y. N., "Old know — how in helix TWT development in the USSR," *AIP Conference Proceeding*, Vol. 691, No. 1, 112–122, Dec. 2003.
7. Kuntzmann, J. C., R. Nazet, and L. Tarreau, "Traveling wave tube comprising a sleeve cut with grooves and its manufacturing process," USA Patent No. 4572985, Feb. 1986.
8. Dayton, J. A., G. T. Mearini, H. Chen, and C. L. Kory, "Diamonded-studded helical traveling wave tube," *IEEE Trans. Electron Devices*, Vol. 52, No. 5, 695–701, May 2005.
9. Henry, D., N. Santonja, and S. Wartski, "Brazed-helix technology for 30 GHz power TWTs," *1986 International Electron Devices Meeting Technical Digest*, Vol. 36, 505–507, 1986.
10. Wartski, S., D. Henry, and N. Santonjia, "Development of a brazed-helix TWT for future Ka-band earth stations delivering 200 W in the band 27.5–30 GHz," *1988 International Electron Devices Meeting Technical Digest*, 366–369, 1988.
11. Gong, Y., Y. Wei, W. Wang, and Z. Duan, "Analysis of a novel brazed helix tape slow wave structure with high power capability," *30th IEEE International Conference on Plasma Science*, 177, 2003.
12. Han, Y., Y. W. Liu, Y. G. Ding, and P. K. Liu, "Improvement of heat dissipation capability of slow-wave structure using two assembling methods," *IEEE Electron Devices Letters*, Vol. 29, No. 8, 955–956, Aug. 2008.

13. Han, Y., Y. Liu, Y. Ding, P. Liu, and C. Lu, "Thermal analysis of a helix TWT slow-wave structure," *IEEE Trans. Electron Devices*, Vol. 55, No. 5, 1269–1272, May 2008.
14. Han, Y., Y. Liu, Y. Ding, and P. Liu, "Reliability analysis of thermal conduction of slow-wave structures assembled with different methods," *IEEE Trans. Electron Devices*, Vol. 9, No. 2, 265–268, May 2009.
15. Jung, S. S., A. V. Soukhov, B. F. Jia, and G. S. Park, "Positive phase-velocity tapering of broadband helix traveling-wave tubes for efficiency enhancement," *Applied Physics Letters*, Vol. 80, No. 16, 3000–3002, Apr. 2002.
16. Ghosh, T. K., A. J. Challis, A. Jacob, D. Bowler, and R. G. Carter, "Improvement in performance of broadband helix traveling-wave tubes," *IEEE Trans. Electron Devices*, Vol. 55, No. 2, 668–673, Feb. 2008.
17. Srivastava, V., R. G. Carter, B. Ravinder, A. K. Sina, and S. N. Joshi, "Design of helix slow-wave structure for high efficiency TWTs," *IEEE Trans. Electron Devices*, Vol. 47, No. 12, 2438–2443, Dec. 2000.
18. Ghosh, T. K., A. J. Challis, A. Jacob, and D. Bowler, "Design of helix pitch profile for broadband traveling-wave tubes," *IEEE Trans. Electron Devices*, Vol. 56, No. 5, 1135–1140, May 2009.
19. Gong, Y., Z. Duan, Y. Wang, Y. Wei, H. Yin, and W. Wang, "Suppression of in-band power holes in helix traveling-wave tubes," *IEEE Trans. Electron Devices*, Vol. 58, No. 5, 1556–1561, May 2011.
20. Wei, Y. Y., L. W. Liu, Y. B. Gong, X. Xu, H. R. Yin, L. N. Yue, Y. Liu, J. Xu, and W. X. Wang, "Helical slow-wave structure," USA Patent Application, No. 13/345, 121, Jan. 2012.
21. Liu, L., Y. Wei, X. Xu, F. Shen, G. Zhao, M. Huang, T. Tang, W. X. Wang, and Y. Gong, "A novel helical slow-wave structure for millimeter wave traveling wave tube," *5th Global Symposium on Millimeter Waves Conference*, 312–315, 2012.
22. Liu, L., Y. Wei, J. Xu, Z. Lu, H. Yin, L. Yue, H. Gong, G. Zhao, Z. Duan, W. Wang, and Y. Gong, "A novel slotted helix slow-wave structure for millimeter-wave traveling-wave tube," *Progress In Electromagnetics Research*, Vol. 135, 347–362, 2013.
23. Booske, J. H., M. C. Converse, C. L. Kory, C. T. Chevalier, D. A. Gallagher, K. E. Kreischer, V. O. Heinen, and S. Bhattacharjee, "Accurate parametric modeling of folded waveguide circuits for millimeter wave traveling wave tubes," *IEEE Trans. Electron Devices*, Vol. 52, No. 5, 685–694, May 2005.

24. Ansoft Corp., "Ansoft HFSS user's reference," Online Available: http://www.ansoft.com.cn/.
25. Ghosh, S., P. K. Jain, and B. N. Basu, "Rigorous tape analysis of inhomogeneously-loaded helical slow-wave structures," *IEEE Trans. Electron Devices*, Vol. 44, No. 7, 1158–1168, Jul. 1997.
26. Liu, S. G., H. F. Li, W. X. Wang, and Y. L. Mo, *Introduction of Microwave Electronics,* 105, National Defence Industry Press, Beijing, China, Sep. 1985.
27. CST Corp., "CST MWS tutorials," Online Available: http://www.cst-china.cn/.
28. CST Corp., "CST PS tutorials," Online Available: http://www.cst-china.cn/.
29. Chong, C. K., R. C. Dawson, J. W. Forster, R. H. Le Borgne, M. L. Ramay, R. J. Stolz, and R. N. Tamashiro, "Development of 500 W Ka-band helix-TWT and 200 W Q-band helix-TWT for communications applications," *Proc. IEEE International Vacuum Electronics Conference*, 191–192, 2008.
30. Bosch, E., R. Christ, M. Lefevre, J. Racamier, H. Rupp, J. Tribout, and J. Jarno, "New 500 W Ka band TWT's," *Proc. IEEE International Vacuum Electronics Conference*, 70–71, 2009.